Progress In Electromagnetics Research, Vol. 167, 1–10, 2020

Shielding of an Imperfect Metallic Thin Circular Disk: Exact and Low-Frequency Analytical Solution

Giampiero Lovat[1, *], Paolo Burghignoli[2], Rodolfo Araneo[1], Salvatore Celozzi[1], Amedeo Andreotti[3], Dario Assante[4], and Luigi Verolino[3]

Abstract—The problem of evaluating the shielding effectiveness of a thin metallic circular disk with finite conductivity against an axially symmetric vertical magnetic dipole is addressed. First, the thin metallic disk is modeled through an appropriate boundary condition, and then, as for the perfectly conducting counterpart, the problem is reduced to a set of dual integral equations which are solved in an exact form through the application of the Galerkin method in the Hankel transform domain. A second-kind Fredholm infinite matrix-operator equation is obtained by selecting a suitable set of basis functions. A low-frequency solution is finally extracted in a closed form. Through a comparison with results obtained from a full-wave commercial software, it is shown that such a simple approximate solution is accurate up to the frequency where the surface-impedance model of the thin disk is valid.

1. INTRODUCTION

The scattering of electromagnetic waves by circular metal disks and their penetration through circular apertures cut in an infinite metal plate constitute a canonical problem in electromagnetic theory and, as such, have been the subject of an intensive research thorough the years, although most of the studies were directed to perfectly-conducting (PEC) and infinitesimally-thin objects (see, e.g., [1–17] and references therein).

Recently, the interaction of an infinitesimally thin PEC disk and a vertical magnetic point source (representing a small electric loop current) has been deeply investigated [18] obtaining the exact representation for the electromagnetic field, valid for any frequency range, through the solution of a set of dual integral equations by means of a numerical Galerkin Method-of-Moments approach and an analytical-regularization scheme. Moreover, surprisingly, a static solution has been obtained in a closed form which has been shown to be accurate up to very high frequencies.

In this work, we extend the analysis presented in [18] by still considering the interaction of a Vertical Magnetic Dipole (VMD) with a circular metallic disk, but having a finite conductivity and a finite thickness. It is worth noting that such a configuration has received much less attention than its ideal counterpart [13, 19–21].

The formulation of the problem, together with the fundamental assumption of thin disk, is first presented in Section 2 and, operating in the Hankel transform domain, a set of dual integral equations is derived. In Section 3, an exact numerical solution is obtained through a Galerkin Method-of-Moments approach pointing out the crucial physical and mathematical differences with respect to the PEC case, whose static solution can be recovered but paying great attention to the limiting process, as shown in

Received 9 September 2019, Accepted 2 December 2019, Scheduled 18 January 2020

* Corresponding author: Giampiero Lovat (giampiero.lovat@uniroma1.it).

[1] Department of Astronautical, Electrical, and Energetic Engineering, Sapienza University of Rome, Italy. [2] Department of Information Engineering, Electronics and Telecommunications, Sapienza University of Rome, Italy. [3] Department of Electrical Engineering and Information Technology, University of Naples "Federico II", Italy. [4] Faculty of Engineering, International Telematic University UniNettuno, Italy.

Section 4. The static-PEC solution is then the base to construct a low-frequency approximate solution in Section 5 whose limits of validity are also discussed. Finally, the conclusions of the work are drawn in Section 6.

2. FORMULATION OF THE PROBLEM

The configuration under analysis consists of a thin metallic circular disk of thickness d and radius a characterized by a finite (bulk) conductivity σ and placed on the plane $z = 0$ of a cylindrical coordinate system (ρ, ϕ, z) with center at the origin and a vertical magnetic dipole (VMD) with magnetic dipole moment m_z placed along the z axis at a height $z = h$ (see Fig. 1). The electromagnetic problem is axial-symmetric so that all the fields depend only on ρ and z. Time-harmonic sources and fields are assumed with an implicit $e^{j\omega t}$ dependence.

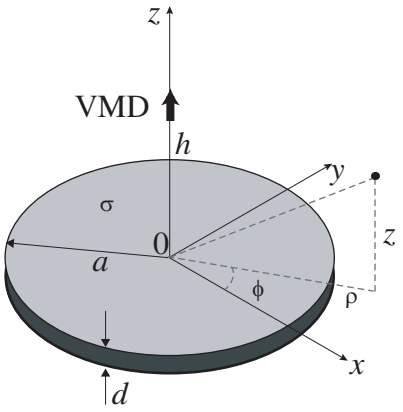

Figure 1. Configuration under analysis: a vertical magnetic dipole (VMD) radiates in the presence of a circular metallic disk with radius a, thickness d, and conductivity σ. The VMD is axially symmetric with respect to the disk and placed at a distance h from it.

As already shown in [18], the incident electric field produced by a vertical magnetic dipole of moment m_z and placed at $z = h$ is

$$E_\phi^{\text{inc}}(\rho, z) = -\frac{k_0 \zeta_0 m_z}{4\pi} \int_0^\infty \frac{e^{-jk_z|z-h|}}{k_z} J_1(k_\rho \rho)\, k_\rho^2 \mathrm{d}k_\rho \tag{1}$$

where k_0 and ζ_0 are the free-space wavenumber and impedance, respectively, and $k_z = \sqrt{k_0^2 - k_\rho^2}$. On the other hand, the electric field scattered by the disk is [18]

$$E_\phi^{\text{scat}}(\rho, z) = -\frac{k_0 \zeta_0}{2} \int_0^\infty \tilde{J}_{S\phi}(k_\rho) \frac{e^{-jk_z|z|}}{k_z} J_1(k_\rho \rho)\, k_\rho \mathrm{d}k_\rho \tag{2}$$

where $\tilde{J}_{S\phi}(k_\rho)$ is the Hankel transform of order 1 [22] of the induced surface current density $J_{S\phi}(\rho)$, with the latter being expressed in A/m.

Provided that the thickness d is less than twice of the skin depth $\delta = 1/\sqrt{\pi \mu_0 \sigma f}$, the following boundary condition on the disk can be assumed [23, 24]:

$$E_\phi^{\text{scat}}(\rho, z = 0) + E_\phi^{\text{inc}}(\rho, z = 0) = R_0 J_{S\phi}(\rho) \tag{3}$$

where

$$R_0 = 1/(\sigma d) \tag{4}$$

is the surface (transition) resistance of the disk. Equations (3) and (4) represent an accurate model up to the frequency $f_{\max} = 2/(\pi \mu_0 \sigma d^2)$ when the skin depth δ is equal to half disk thickness $d/2$. By

assuming the boundary condition in Eqs. (3)–(4), the following set of dual integral equations can be derived:

$$\begin{aligned} &-k_0\zeta_0\int_0^\infty \frac{1}{2k_z}\left(\tilde{J}_{S\Phi}(k_\rho)+\frac{m_z k_\rho}{2\pi}e^{-jk_z h}\right)J_1\left(k_\rho\rho\right)k_\rho \mathrm{d}k_\rho = R_0 J_{S\phi}(\rho)\,, \quad \rho<a \\ &\int_0^\infty \tilde{J}_{S\phi}\left(k_\rho\right)J_1\left(k_\rho\rho\right)k_\rho \mathrm{d}k_\rho = 0\,, \qquad\qquad \rho>a \end{aligned} \tag{5}$$

where the second equation enforces the vanishing of $J_{S\Phi}(\rho)$ outside the disk.

3. GALERKIN METHOD-OF-MOMENTS SOLUTION

By expressing the surface current density $J_{S\phi}(\rho)$ as an inverse Hankel transform and rearranging some terms, the first equation in Eq. (5) can be rewritten as

$$\int_0^\infty \left(\frac{k_0\zeta_0}{2R_0k_z}+1\right)\tilde{J}_{S\Phi}(k_\rho)J_1\left(k_\rho\rho\right)k_\rho \mathrm{d}k_\rho = -\int_0^\infty \frac{k_0\zeta_0}{R_0k_z}\frac{m_z k_\rho}{4\pi}e^{-jk_z h}J_1\left(k_\rho\rho\right)k_\rho \mathrm{d}k_\rho \tag{6}$$

We can expand the unknown surface current density through a set of basis functions $b_n(\rho)$ whose Hankel transform is $\tilde{b}_n(k_\rho)$ so that

$$J_{S\phi}\left(\rho\right)=\sum_{n=1}^{+\infty} i_n b_n\left(\rho\right) \tag{7}$$

and

$$\tilde{J}_{S\phi}\left(k_\rho\right)=\sum_{n=1}^{+\infty} i_n \tilde{b}_n\left(k_\rho\right) \tag{8}$$

By applying the Galerkin Method of Moments, we obtain the algebraic system

$$\sum_{n=1}^{N} A_{mn}^{\sigma} i_n = B_m^{\sigma}, \quad m=1,\ldots,N \tag{9}$$

where

$$A_{mn}^{\sigma}=\frac{k_0\zeta_0}{2R_0}\int_0^\infty \frac{\tilde{b}_m\left(k_\rho\right)\tilde{b}_n\left(k_\rho\right)}{k_z}k_\rho \mathrm{d}k_\rho + \int_0^\infty \tilde{b}_m\left(k_\rho\right)\tilde{b}_n\left(k_\rho\right)k_\rho \mathrm{d}k_\rho \tag{10}$$

and

$$B_m^{\sigma}=-\frac{k_0\zeta_0 m_z}{4\pi R_0}\int_0^\infty \tilde{b}_m\left(k_\rho\right)\frac{k_\rho^2}{k_z}e^{-jk_z h}\mathrm{d}k_\rho \tag{11}$$

The presence of a finite conductivity σ deeply changes the nature of the problem with respect to the perfectly conducting (PEC) case [18]: in fact, the static limit for $R_0 \neq 0$ produces a current which is identically zero. Moreover, the finite conductivity implies that the current is not singular anymore at the edges of the disk [25]. Therefore, the following set of basis functions is adopted [26]:

$$b_n\left(\rho\right)=\begin{cases} 0 & \rho>a \\ \dfrac{\rho}{a^2}P_{n-1}^{(1,0)}\left(1-2\dfrac{\rho^2}{a^2}\right), \quad n=1,2,\ldots & \rho<a \end{cases} \tag{12}$$

where $P_n^{(\alpha,\beta)}(\cdot)$ are the Jacobi polynomials of order n. The Hankel transforms of Eq. (12) are

$$\tilde{b}_n\left(k_\rho\right)=\int_0^a \frac{\rho}{a^2}P_{n-1}^{(1,0)}\left(1-2\frac{\rho^2}{a^2}\right)J_1\left(k_\rho\rho\right)\rho \mathrm{d}\rho = \frac{J_{2n}\left(k_\rho a\right)}{k_\rho} \tag{13}$$

By adopting this set of basis functions, from Eq. (10), we obtain

$$A_{mn}^{\sigma}=\frac{k_0\zeta_0}{2R_0}\int_0^\infty \frac{J_{2m}\left(k_\rho a\right)J_{2n}\left(k_\rho a\right)}{k_\rho\sqrt{k_0^2-k_\rho^2}}\mathrm{d}k_\rho + \int_0^\infty \frac{J_{2m}\left(k_\rho a\right)J_{2n}\left(k_\rho a\right)}{k_\rho}\mathrm{d}k_\rho \tag{14}$$

Taking into account the integral identity [27, 6.574]

$$\int_0^\infty J_\nu(\alpha t)J_\mu(\alpha t)t^{-\lambda}\mathrm{d}t = \frac{\alpha^{\lambda-1}\Gamma(\lambda)\,\Gamma\left(\dfrac{\nu+\mu-\lambda+1}{2}\right)}{2^\lambda\Gamma\left(\dfrac{-\nu+\mu+\lambda+1}{2}\right)\Gamma\left(\dfrac{\nu+\mu+\lambda+1}{2}\right)\Gamma\left(\dfrac{\nu-\mu+\lambda+1}{2}\right)} \tag{15}$$

valid for $\nu+\mu+1>\lambda>0$ and $\alpha>0$, by letting $\nu=2m-1/2$, $\mu=2n-1/2$, $\alpha=a$, $t=k_\rho$, and $\lambda=1$, we have

$$\int_0^\infty \frac{J_{2m}(k_\rho a)\,J_{2n}(k_\rho a)}{k_\rho}\mathrm{d}k_\rho = \frac{\Gamma(1)\Gamma(n+m)}{2\Gamma(m-n+1)\,\Gamma(n+m+1)\,\Gamma(n-m+1)} = \frac{\delta_{mn}}{4m} \tag{16}$$

and therefore

$$A^\sigma_{mn} = \frac{k_0\zeta_0}{2R_0}\int_0^\infty \frac{J_{2m}(k_\rho a)\,J_{2n}(k_\rho a)}{k_\rho\sqrt{k_0^2-k_\rho^2}}\mathrm{d}k_\rho + \frac{\delta_{mn}}{4m} \tag{17}$$

where δ_{mn} is the Kronecker symbol. Moreover

$$B^\sigma_m = -\frac{k_0\zeta_0 m_z}{4\pi R_0}\int_0^\infty J_{2m}(k_\rho a)\,k_\rho\frac{e^{-j\sqrt{k_0^2-{k_\rho}^2}h}}{\sqrt{k_0^2-k_\rho^2}}\mathrm{d}k_\rho \tag{18}$$

It is worth noting that, thanks to the particular choice of the basis functions which diagonalize the perturbative term due to the finite conductivity, in the limit $N\to+\infty$ the system in Eq. (9) can be rewritten as

$$i_m + \sum_{n=1}^\infty \hat{A}^\sigma_{mn} i_n = \hat{B}^\sigma_m \tag{19}$$

where

$$\hat{A}^\sigma_{mn} = \frac{2mk_0\zeta_0}{R_0}\int_0^\infty \frac{J_{2m}(k_\rho a)\,J_{2n}(k_\rho a)}{k_\rho\sqrt{k_0^2-k_\rho^2}}\mathrm{d}k_\rho \tag{20}$$

and

$$\hat{B}^\sigma_m = -\frac{mk_0\zeta_0 m_z}{\pi R_0}\int_0^\infty J_{2m}(k_\rho a)\,k_\rho\frac{e^{-j\sqrt{k_0^2-{k_\rho}^2}h}}{\sqrt{k_0^2-k_\rho^2}}\mathrm{d}k_\rho \tag{21}$$

Remarkably, Eq. (19) is a second-kind Fredholm equation in the space ℓ_2 of the square-summable sequences; as such, it does not require any regularization scheme [10]. Therefore, compared with the PEC case [18], the finite conductivity has the role of a regularizing parameter. The fact that the integral equation is Fredholm second-kind type guarantees that a unique solution exists, which can be obtained through any discretization or truncation scheme.

The integral in Eq. (20) can be expressed through a rapidly convergent series thanks to the identity [28]

$$(-1)^{l'-l}\,2k\int_0^\infty \frac{J_{|m|+2l+1}(\tau a)\,J_{|m|+2l'+1}(\tau a)}{\tau\sqrt{k^2-\tau^2}}\mathrm{d}\tau = -\sum_{l=1}^\infty \frac{\left(-\dfrac{1}{2}l\right)_p\left(-\dfrac{1}{2}l+1\right)_q(-jka)^l}{\Gamma\left(\dfrac{1}{2}l+p+1\right)\Gamma\left(\dfrac{1}{2}l+q+2\right)} \tag{22}$$

with $p=l'-l$, $q=|m|+l'+l$, and where $(x)_y$ is the Pochhammer symbol defined as

$$(x)_y = \frac{\Gamma(x+y)}{\Gamma(x)} \tag{23}$$

In fact, by letting $k = k_0$, $\tau = k_\rho$, $l = m-1$, $l' = n-1$, $m = 1$ and therefore $p = n-m$ and $q = n+m-1$ in Eq. (22), from Eq. (20) we have

$$\hat{A}^{\sigma}_{mn} = (-1)^{p+1} \frac{m\zeta_0}{R_0} \sum_{l=1}^{\infty} \frac{\left(-\frac{1}{2}l\right)_p \left(-\frac{1}{2}l+1\right)_q (-jk_0a)^l}{\Gamma\left(\frac{1}{2}l+p+1\right)\Gamma\left(\frac{1}{2}l+q+2\right)} \tag{24}$$

Once the coefficients i_n have been determined, the scattered magnetic field can readily be found as

$$\begin{aligned} H_\rho^{\text{scat}}(\rho,z) &= \sum_{n=1}^{N} \frac{i_n}{2} \int_0^\infty \tilde{b}_n(k_\rho)\, e^{-jk_z|z|} J_1(k_\rho\rho)\, k_\rho \mathrm{d}k_\rho \\ &= \sum_{n=1}^{N} \frac{i_n}{2} \int_0^\infty J_{2n}(k_\rho a)\, J_1(k_\rho\rho)\, e^{-j\sqrt{k_0^2-k_\rho^2}|z|} \mathrm{d}k_\rho \end{aligned} \tag{25}$$

and

$$\begin{aligned} H_z^{\text{scat}}(\rho,z) &= -j \sum_{n=1}^{N} \frac{i_n}{2} \int_0^\infty \tilde{b}_n(k_\rho) \frac{e^{-jk_z|z|}}{k_z} {k_\rho}^2 J_0(k_\rho\rho)\, \mathrm{d}k_\rho \\ &= -j \sum_{n=1}^{N} \frac{i_n}{2} \int_0^\infty J_{2n}(k_\rho a)\, J_0(k_\rho\rho)\, k_\rho \frac{e^{-j\sqrt{k_0^2-k_\rho^2}|z|}}{\sqrt{k_0^2-k_\rho^2}} \mathrm{d}k_\rho \end{aligned} \tag{26}$$

4. STATIC LIMIT OF THE PEC CASE

It is possible to obtain the static limit of the PEC case by first letting $R_0 = 0$ (PEC condition) and next letting $k_0 = 0$. In fact, it should be noted that one cannot recover the static solution of the PEC case if the two limits are inverted, i.e., if the static condition $k_0 = 0$ is first enforced and next the PEC condition $R_0 = 0$: in such a case, the trivial identically zero solution is obtained. Such a situation is typical of a singular perturbation [29]. To this aim, by multiplying all the elements of the system in Eq. (19) by the factor $2R_0/(k_0\zeta_0)$, then letting $R_0 = 0$, and finally $k_0 = 0$ we obtain

$$\sum_{n=1}^{\infty} \hat{A}^{(0)}_{mn} i_n = \hat{B}^{(0)}_m \tag{27}$$

where

$$\hat{A}^{(0)}_{mn} = j \int_0^\infty \frac{J_{2m}(k_\rho a)\, J_{2n}(k_\rho a)}{k_\rho^2} \mathrm{d}k_\rho \tag{28}$$

and

$$\hat{B}^{(0)}_m = -j \frac{m_z}{2\pi} \int_0^\infty J_{2m}(k_\rho a)\, e^{-k_\rho h} \mathrm{d}k_\rho \tag{29}$$

All the elements can be evaluated in a closed form by using the identities in Eq. (15) and [27, 6.611]

$$\int_0^\infty e^{-\alpha x} J_\nu(\beta x)\, \mathrm{d}x = \frac{\beta^{-\nu}\left[\sqrt{\alpha^2+\beta^2}-\alpha\right]^\nu}{\sqrt{\alpha^2+\beta^2}} \tag{30}$$

thus obtaining

$$\hat{A}^{(0)}_{mn} = ja \frac{\Gamma\left(\frac{2m+2n-1}{2}\right)}{4\Gamma\left(\frac{2m-2n+3}{2}\right)\Gamma\left(\frac{2n-2m+3}{2}\right)\Gamma\left(\frac{2m+2n+3}{2}\right)} \tag{31}$$

Thanks to the property of the Gamma function

$$\Gamma(z+1) = z\Gamma(z) \tag{32}$$

Eq. (31) can also be expressed as

$$\hat{A}_{mn}^{(0)} = ja\frac{\left(m+n-\frac{1}{2}\right)\left(m+n+\frac{1}{2}\right)}{4\Gamma\left(\frac{2m-2n+3}{2}\right)\Gamma\left(\frac{2n-2m+3}{2}\right)} \tag{33}$$

and moreover

$$\hat{B}_{m}^{(0)} = -j\frac{m_z}{2\pi}\frac{\left[\sqrt{1+\frac{h^2}{a^2}}-\frac{h}{a}\right]^{2m}}{\sqrt{a^2+h^2}} \tag{34}$$

From Eqs. (25)–(26), the scattered magnetic field can be expressed in the static limit as

$$H_{\rho}^{\text{scat}}(\rho,z) = \frac{1}{2}\sum_{n=1}^{N} i_n \int_0^{\infty} J_{2n}(k_\rho a)\, J_1(k_\rho \rho)\, e^{-k_\rho |z|}\mathrm{d}k_\rho \tag{35}$$

$$H_{z}^{\text{scat}}(\rho,z) = \frac{1}{2}\sum_{n=1}^{N} i_n \int_0^{\infty} J_{2n}(k_\rho a)\, J_0(k_\rho \rho)\, e^{-k_\rho |z|}\mathrm{d}k_\rho \tag{36}$$

By using the identity [27, 6.626]

$$\int_0^{\infty} x^{\lambda-1}e^{-\alpha x}J_\mu(\beta x)J_\nu(\gamma x)\mathrm{d}x = \frac{\beta^\mu\gamma^\nu}{\Gamma(\nu+1)}2^{-\nu-\mu}\alpha^{-\lambda-\mu-\nu} \cdot\sum_{m=0}^{\infty}\frac{\Gamma(\lambda+\mu+\nu+2m)}{m!\Gamma(\mu+m+1)}F\left(-m,-\mu-m;\nu+1;\frac{\gamma^2}{\beta^2}\right)\left(-\frac{\beta^2}{4\alpha^2}\right)^m \tag{37}$$

valid for $\lambda+\mu+\nu>0$ and $\alpha>0$, where $F(\cdot,\cdot;\cdot;\cdot)$ are the Gauss hypergeometric functions, we obtain

$$H_{\rho}^{\text{scat}}(\rho,z) = \rho\sum_{n=1}^{N} i_n \frac{a^{2n}}{(2|z|)^{2n+2}}\sum_{m=0}^{\infty}\frac{(2n+2m+1)!}{m!(2n+m)!}F\left(-m,-2n-m;2;\frac{\rho^2}{a^2}\right)\left(-\frac{a^2}{4|z|^2}\right)^m \tag{38}$$

and

$$H_{z}^{\text{scat}}(\rho,z) = \sum_{n=1}^{N} i_n \frac{a^{2n}}{(2|z|)^{2n+1}}\sum_{m=0}^{\infty}\frac{(2n+2m)!}{m!(2n+m)!}F\left(-m,-2n-m;1;\frac{\rho^2}{a^2}\right)\left(-\frac{a^2}{4|z|^2}\right)^m \tag{39}$$

The scattered field is thus expressed through integrals of Lipschitz-Hankel kind for which different representations exist in terms of first- and second-kind elliptic integrals [30].

It is worth noting that for $\rho=0$, we have $H_{\rho}^{\text{scat}}=0$ and

$$H_{z}^{\text{scat}}(0,z) = \frac{1}{2}\sum_{n=1}^{N} i_n \int_0^{\infty} J_{2n}(k_\rho a)\, e^{-k_\rho |z|}\mathrm{d}k_\rho \tag{40}$$

i.e., by using the identity in Eq. (30)

$$H_{z}^{\text{scat}}(0,z) = \frac{1}{2}\sum_{n=1}^{N} i_n \frac{\left[\sqrt{1+\frac{|z|^2}{a^2}}-\frac{|z|}{a}\right]^{2n}}{\sqrt{a^2+|z|^2}} \tag{41}$$

The proposed formulation is exact, but since the adopted basis functions do not automatically take into account the algebraic singular behavior at the edges of the disk present in the PEC case the convergence is worse with respect to the formulation presented in [18]. In Fig. 2, the behavior of the current density and of the scattered magnetic field for a PEC disk is presented as a function of the number of basis functions for the same configuration considered in [18] (i.e., $a=5\,\text{cm}$ and $h/a=2$).

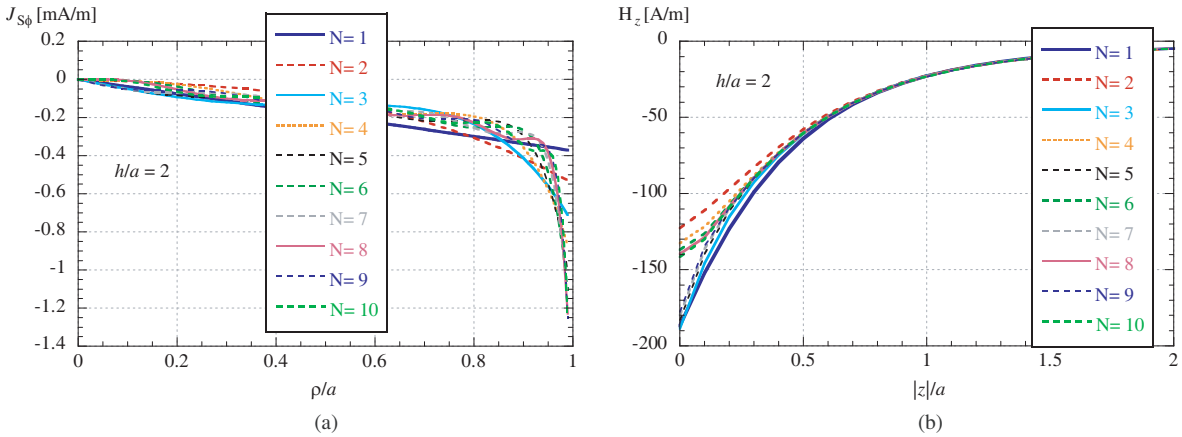

Figure 2. Convergence of the surface current density and of the scattered magnetic field as a function of the number N of basis functions for a PEC disk. *Parameters*: $m_z = 1\,\mathrm{Am}^2$, $a = 5\,\mathrm{cm}$, $h/a = 2$.

5. LOW-FREQUENCY APPROXIMATION

In order to obtain a low-frequency approximation for the problem of a disk with a finite conductivity, one can think to use the static integral of the PEC case with a perturbative term dependent on frequency which takes into account the finite conductivity of the disk. To this aim, the integrals in Eq. (19) are approximated with their static version so that the system to be solved is

$$i_m + \sum_{n=1}^{\infty} \hat{A}_{mn}^{\sigma(0)} i_n = \hat{B}_m^{\sigma(0)} \tag{42}$$

where

$$\hat{A}_{mn}^{\sigma(0)} = \frac{2mk_0\zeta_0}{R_0} \hat{A}_{mn}^{(0)} \tag{43}$$

and

$$\hat{B}_m^{\sigma(0)} = \frac{2mk_0\zeta_0}{R_0} \hat{B}_m^{(0)} \tag{44}$$

Once the coefficients i_n have been obtained, the scattered field is calculated through the static formulas (35)–(36): in particular, for the scattered field along the dipole and disk axis, and Eq. (41) is used.

It is interesting to compare the magnetic shielding effectiveness [31] obtained with a full-wave formulation and that obtained with the low-frequency approximation. The magnetic shielding effectiveness along the axis z is defined as

$$\mathrm{SE}_H = 20 \log \frac{\left|H_z^{\mathrm{inc}}(0,z)\right|}{\left|H_z^{\mathrm{tot}}(0,z)\right|} \tag{45}$$

where $H_z^{\mathrm{tot}} = H_z^{\mathrm{inc}} + H_z^{\mathrm{scat}}$.

An example is reported in Fig. 3, where a configuration with $h = 30\,\mathrm{cm}$, $z = -h$, $\sigma = 5.7 \cdot 10^7\,\mathrm{S/m}$ (copper disk), $d = 1\,\mathrm{mm}$ is considered. Different values of radius are considered, and the infinite planar case (i.e., for $a \to +\infty$) is also reported as [32].

In particular, the full-wave problem has been solved in the frequency domain by means of a two-dimensional (2-D) axially symmetric FEM, i.e., the low-frequency magnetic-field package of the commercial software COMSOL. As far as the FEM discretization is concered, third-order triangular Lagrangian elements have been used, and infinite elements to truncate the computational domain have been introduced [33]. Moreover, the volume of the screen is discretized with an appropriate boundary-layer mesh in order to accurately account for the diffusion effects inside the screen and adequately resolve the penetration depth of the induced currents [34].

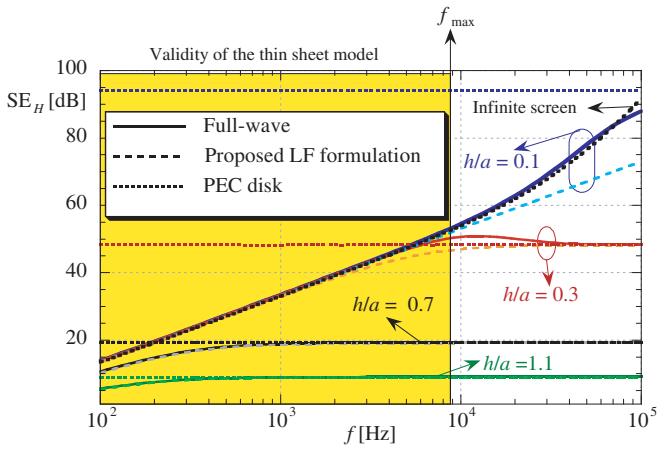

Figure 3. Magnetic shielding effectiveness SE_H of a copper disk as a function of frequency f for different values of h/a: comparison between the proposed low-frequency formulation and a full-wave solution. Solution for the PEC disk is also reported as reference. *Parameters*: $h = 30\,\mathrm{cm}$, $z = -h$, $\sigma = 5.7 \cdot 10^7\,\mathrm{S/m}$, $d = 1\,\mathrm{mm}$.

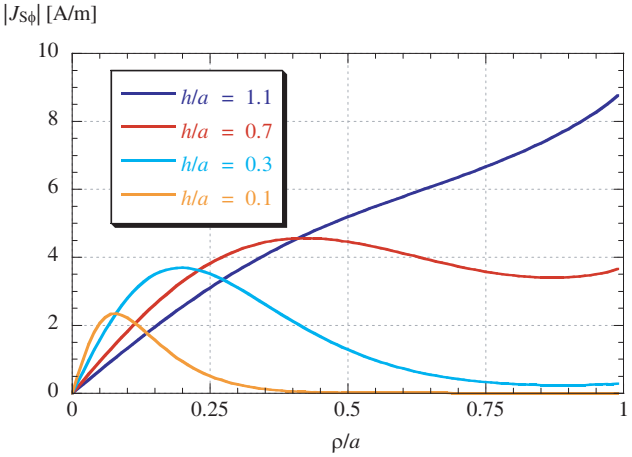

Figure 4. Absolute value of the surface current density as a function of ρ/a for different values of h/a. *Parameters*: $f = 1\,\mathrm{kHz}$, $h = 30\,\mathrm{cm}$, $\sigma = 5.7 \cdot 10^7\,\mathrm{S/m}$, $d = 1\,\mathrm{mm}$, $m_z = 1\,\mathrm{Am}^2$.

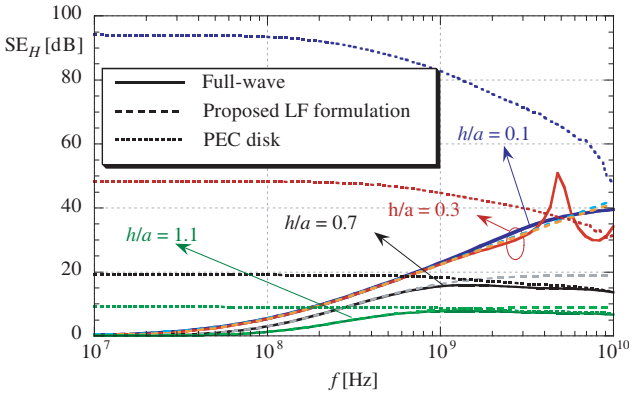

Figure 5. Magnetic shielding effectiveness SE_H of a conductive-painting disk as a function of frequency f for different values of h/a: comparison between the proposed low-frequency formulation and a full-wave solution. Solution for the PEC disk is also reported as reference. *Parameters*: $h = 1\,\mathrm{cm}$, $z = -h$, $\sigma = 5 \cdot 10^3\,\mathrm{S/m}$, $d = 0.1\,\mathrm{mm}$.

It can be seen that the low-frequency approximation is an excellent representation of the exact solution over the whole frequency range within which the finite-conductivity disk can be represented as an infinitesimally thin sheet of surface resistance R_0, i.e., for the adopted screen parameters, up to the frequency $f_{\max} = 8.8 \cdot 10^3\,\mathrm{Hz}$. For comparison purposes, in Fig. 3 the relevant solutions for a PEC disk are also reported. As expected, in the low-frequency regime, the SE_H of the lossy configuration is smaller than the relevant PEC performance, which however represents the asymptotic result for high frequencies. An exception to such a behavior is represented by the case $h/a = 0.3$ in an intermediate frequency region where the SE_H of the lossy configuration is larger than that for the PEC disk because of a resonance effect [34].

It is also interesting to observe the variation of the surface density current as a function of the

radius a for a fixed value of h and at a certain operating frequency, according to Eqs. (7) and (9). An example is reported in Fig. 4, where $h = 30\,\text{cm}$ and $f = 1\,\text{kHz}$. As expected, with respect to the PEC case, the surface current density does not present any singular behavior at the edges.

As a second example, a disk of conductive painting characterized by a conductivity $\sigma = 5 \cdot 10^3\,\text{S/m}$ and a thickness $d = 0.1\,\text{mm}$. The source is placed at $h = 1\,\text{cm}$ and the observation point at $z = -h$. The relevant magnetic shielding effectiveness SE_H is reported in Fig. 5 as a function of frequency and for different values of the radius a. Both the proposed low-frequency approximation and a full-wave solution are reported for comparison. It is worth noting that, for the adopted values of conductivity and thickness, the thin-sheet approximation is valid in the entire considered frequency range (in fact $f_{\max} = 1.01 \cdot 10^{10}\,\text{Hz}$): although not shown, the results obtained through Eq. (26) and the commercial software COMSOL are completely superimposed. On the other hand, the proposed low-frequency representation is correct up to the frequency $f = 1 \cdot 10^9\,\text{Hz}$ beyond which other resonance effects, depending on the disk radius, may occur [34]. In this case, because of the much lower value of the conductivity than the copper case, the difference with respect to the relevant PEC disk is much more pronounced although, for high frequencies, the PEC case still represents the limiting solution.

6. CONCLUSION

The problem of radiation by a vertical magnetic dipole in the presence of a thin metallic circular disk with finite conductivity has been addressed. Modeling the thin conductive disk through an appropriate boundary condition, the problem is reduced to the solution of a set of dual integral equations. The latter is exactly solved through the application of the Galerkin method in the Hankel transform domain. A low-frequency solution is extracted in a closed form and is shown to be very accurate up to the frequency where the surface-impedance model of the thin disk is valid.

REFERENCES

1. Bethe, H. A., "Theory of diffraction by small holes," *Physical Review*, Vol. 66, Nos. 7–8, 163, 1944.
2. Bouwkamp, C., "On the diffraction of electromagnetic waves by small circular disks and holes," *Philips Research Reports*, Vol. 5, 401–422, 1950.
3. Flammer, C., "The vector wave function solution of the diffraction of electromagnetic waves by circular disks and apertures. I. Oblate spheroidal vector wave functions," *J. Appl. Phys.*, Vol. 24, No. 9, 1218–1223, 1953.
4. Ehrlich, M. J., S. Silver, and G. Held, "Studies of the diffraction of electromagnetic waves by circular apertures and complementary obstacles: The near-zone field," *J. Appl. Phys.*, Vol. 26, No. 3, 336–345, 1955.
5. Millar, R., "The diffraction of an electromagnetic wave by a circular aperture," *Proc. IEE-Part C: Monographs*, Vol. 104, No. 5, 87–95, 1957.
6. Eggimann, W., "Higher-order evaluation of electromagnetic diffraction by circular disks," *IRE Trans. Microw. Theory Techn.*, Vol. 9, No. 5, 408–418, 1961.
7. Williams, W., "Electromagnetic diffraction by a circular disk," *Proc. Cambridge Phil. Soc.*, Vol. 58, No. 4, 625–630, Cambridge University Press, 1962.
8. Marsland, D., C. Balanis, and S. Brumley, "Higher order diffractions from a circular disk," *IEEE Trans. Antennas Propag.*, Vol. 35, No. 12, 1436–1444, 1987.
9. Duan, D.-W., Y. Rahmat-Samii, and J. P. Mahon, "Scattering from a circular disk: A comparative study of PTD and GTD techniques," *Proc. IEEE*, Vol. 79, No. 10, 1472–1480, 1991.
10. Nosich, A. I., "The method of analytical regularization in wave-scattering and eigenvalue problems: Foundations and review of solutions," *IEEE Antennas Propag. Mag.*, Vol. 41, No. 3, 34–49, 1999.
11. Bliznyuk, N. Y., A. I. Nosich, and A. N. Khizhnyak, "Accurate computation of a circular-disk printed antenna axisymmetrically excited by an electric dipole," *Microw. Opt. Techn. Lett.*, Vol. 25, No. 3, 211–216, 2000.

12. Hongo, K. and Q. A. Naqvi, "Diffraction of electromagnetic wave by disk and circular hole in a perfectly conducting plane," *Progress In Electromagnetics Research*, Vol. 68, 113–150, 2007.
13. Balaban, M. V., R. Sauleau, T. M. Benson, and A. I. Nosich, "Dual integral equations technique in electromagnetic wave scattering by a thin disk," *Progress In Electromagnetics Research B*, Vol. 16, 107–126, 2009.
14. Hongo, K., A. D. U. Jafri, and Q. A. Naqvi, "Scattering of electromagnetic spherical wave by a perfectly conducting disk," *Progress In Electromagnetics Research*, Vol. 129, 315–343, 2012.
15. Di Murro, F., M. Lucido, G. Panariello, and F. Schettino, "Guaranteed-convergence method of analysis of the scattering by an arbitrarily oriented zero-thickness PEC disk buried in a lossy half-space," *IEEE Trans. Antennas Propag.*, Vol. 63, No. 8, 3610–3620, 2015.
16. Nosich, A. I., "Method of analytical regularization in computational photonics," *Radio Sci.*, Vol. 51, No. 8, 1421–1430, 2016.
17. Lucido, M., G. Panariello, and F. Schettino, "Scattering by a zero-thickness PEC disk: A new analytically regularizing procedure based on Helmholtz decomposition and Galerkin method," *Radio Sci.*, Vol. 52, No. 1, 2–14, 2017.
18. Lovat, G., P. Burghignoli, R. Araneo, S. Celozzi, A. Andreotti, D. Assante, and L. Verolino, "Shielding of a perfectly conducting Circular Disk: Exact and Static analytical solution," *Progress In Electromagnetics Research C*, Vol. 95, 167–182, 2019.
19. Roberts, A., "Electromagnetic theory of diffraction by a circular aperture in a thick, perfectly conducting screen," *J. Opt. Soc. Am. A*, Vol. 4, No. 10, 1970–1983, 1987.
20. Lee, H. S. and H. J. Eom, "Electromagnetic scattering from a thick circular aperture," *Microw. Opt. Techn. Lett.*, Vol. 36, No. 3, 228–231, 2003.
21. Balaban, M. V., O. V. Shapoval, and A. I. Nosich, "THz wave scattering by a graphene strip and a disk in the free space: Integral equation analysis and surface plasmon resonances," *J. Opt.*, Vol. 15, No. 11, 114007, 2013.
22. Chew, W. C., *Waves and Fields in Inhomogenous Media*, IEEE Press, Piscataway, NJ, 1999.
23. Bleszynski, E., M. K. Bleszynski, and T. Jaroszewicz, "Surface-integral equations for electromagnetic scattering from impenetrable and penetrable sheets," *IEEE Antennas Propag. Mag.*, Vol. 35, No. 6, 14–25, 1993.
24. Burghignoli, P., G. Lovat, R. Araneo, and S. Celozzi, "Time-domain shielding of a thin conductive sheet in the presence of vertical dipoles," *IEEE Trans. Electromagn. Compat.*, Vol. 60, No. 1, 157–165, Jan. 2018.
25. Farina, M. and T. Rozzi, "Numerical investigation of the field and current behavior near lossy edges," *IEEE Trans. Microw. Theory Tech.*, Vol. 49, No. 7, 1355–1358, 2001.
26. Bliznyuk, N. Y. and A. I. Nosich, "Numerical analysis of a dielectric disk antenna," *Telecommunications and Radio Engineering*, Vol. 61, 273–278, 2004.
27. Gradshteyn, I. S. and I. M. Ryzhik, *Table of Integrals, Series, and Products*, 7th Edition, Academic Press, Burlington, MA, 2014.
28. Rdzanek, W. P., "Sound scattering and transmission through a circular cylindrical aperture revisited using the radial polynomials," *J. Acoust. Soc. Am.*, Vol. 143, No. 3, 1259–1282, 2018.
29. Smith, D. R., *Singular-Perturbation Theory: An Introduction with Applications*, Cambridge University Press, 1985.
30. Eason, G., B. Noble, and I. N. Sneddon, "On certain integrals of Lipschitz-Hankel type involving products of Bessel functions," *Phil. Trans. R. Soc. Lond. A*, Vol. 247, No. 935, 529–551, 1955.
31. Celozzi, S., R. Araneo, and G. Lovat, *Electromagnetic Shielding*, Wiley-IEEE, Hoboken, 2008.
32. Moser, J. R., "Low-frequency low-impedance electromagnetic shielding," *IEEE Trans. Electromagn. Compat.*, Vol. 30, No. 3, 202–210, 1988.
33. Jin, J.-M., *The Finite Element Method in Electromagnetics*, Wiley-IEEE Press, 2014.
34. Araneo, R., G. Lovat, S. Celozzi, and P. Burghignoli, "ELF shielding of finite-size finite-thickness screens against magnetic fields," *2018 IEEE International Conference on EEEIC/I&CPS Europe)*, 1–5, IEEE, 2018.